2008

Analysis and optimization of empirical path loss models and shadowing effects for the Tampa Bay area in the 2.6 GHz band

Julio C. Costa
University of South Florida

Analysis and Optimization of Empirical Path Loss Models and Shadowing Effects for the Tampa Bay Area in the 2.6 GHz Band

by

Julio C. Costa

A thesis submitted in partial fulfillment
of the requirements for the degree of
Master of Science in Electrical Engineering
Department of Electrical Engineering
College of Engineering
University of South Florida

Major Professor: Hüseyin Arslan, Ph.D.
Wilfrido Moreno, Ph.D.
Thomas Weller, Ph.D.

Date of Approval:
March 21, 2008

Keywords: Wireless Communications, Received Signal Strength, Slow Fading, Spatial Correlation, Statistical Regression

DEDICATION

To God for allowing me in this world, to my family for caring for me, to my friends for showing me things around it, and to my wife for making me a better man.

ACKNOWLEDGMENTS

I am forever in debt to Dr. Arslan and the members of the Wireless Communication and Signal Processing Group particularly Hasari Celebi and Serhan Yarkan for their patience and friendship and the knowledge they have shared with me. Dr. Moreno and Dr. Weller have provided me with great feedback for this thesis and I am grateful for their time and insight.

I am very thankful for the opportunity my employer Sprint Nextel has given me, and I am very fortunate to work with my colleagues who have provided me with support and perspectives.

I am also humbled to acknowledge my family and friends for all they have done in my life to get me where I am today.

Finally, I thank God for protecting me in the darkest moments of my life.

"The Lord is my shepherd; I shall not want…" –Psalm 23:1-6

TABLE OF CONTENTS

LIST OF TABLES

LIST OF FIGURES

ANALYSIS AND OPTIMIZATION OF EMPIRICAL PATH LOSS MODELS AND SHADOWING EFFECTS FOR THE TAMPA BAY AREA IN THE 2.6 GHz BAND

Julio C. Costa

ABSTRACT

This thesis analyzes the wireless propagation modeling of a 2.6 GHz band channel around the Tampa Bay area. Different empirical models are compared against measured data, and an adapted model, specific for the Tampa Bay area, is presented that builds on the accuracy of existing models. The effects of the propagation characteristics along bridges are also discussed, and a two-slope model is presented. The proposed models are based on a simple linear regression method, and statistical tests are evaluated for reliability thereof. The analysis also investigates the statistical properties of shadowing effects imposed on the wireless channel. The spatial correlation properties of shadowing effects are investigated in detail, and an extension of existing correlation models for shadowing effects is suggested where the correlation properties are studied in different distance ranges rather than the whole service coverage area.

CHAPTER 1

INTRODUCTION

1.1 Motivation

The advent of Internet has changed the way we communicate and share information. No less significant has been the ubiquity of cellular telephony around the world, particularly in less developed countries. A new paradigm is emerging that promises to bring these two technologies together, an advent that can represent business opportunities and higher quality of life in the underdeveloped world. The technologies that are primed to bring about these changes have been classified as Worldwide Interoperability for Microwave Access (WiMAX) or Long Term Evolution (LTE) under the umbrella of proposed specifications such as beyond 3G or 4G. Even though these specifications have not yet been clearly defined, one commonality within these stages is the frequency band where these specific technologies may be deployed. Therefore it is advantageous to understand how the channel behaves in different environments in order to deploy these new networks in the most cost effective and efficient manner. This thesis analyzes the behavior of the wireless channel in the 2.6 GHz band using data collected from 29 locations around the Tampa Bay area, and it presents an adapted model that provides a better fit than existing models for this specific area. We approach this problem by using a simple linear regression method to describe the path losses of transmitted radio signals in the Tampa Bay area. In addition, shadowing effects are studied and modeled to provide insight into the deployment design of the network as well as in the optimization phase of the system. We then comment on the variance about the mean of the path loss curve and extend on the existing models that describe shadowing effects.

1.2 History

In August of 1997 Sprint Nextel announced it would invest more then $3 billion over the next two years to build a WiMAX network to reach 100 million people in the United States. Sprint Nextel is the largest holder of the 2.6 GHz Broadband Radio Services (BRS) band licenses that cover about 85 percent of the U.S. population. The BRS band is formerly know as the Multipoint Distribution Service (MDS)/Multichannel Multipoint Distribution Service (MMDS). It was originally allocated for the transmission of data and video programming to subscribers using high-powered systems, also known as wireless cable.

In October 1997, the International Telecommunication Union (ITU-R) included WiMAX technology in the IMT-2000 set of standards. This decision may help escalate the opportunities of global deployment in both rural and urban markets to deliver high speed mobile Internet services. These services are mostly likely to be deployed in the 2.6 GHz band. This band is already available for mobile and fixed services in the U.S.

Therefore, the motivation to understand the propagation characteristics of radio link in this band is warranted. In this thesis we will explore the mobile radio propagation characteristics and behaviors in the Tampa Bay area.

1.3 Mobile Radio Propagation

The basic characterization of the propagation of the wireless channel can be described as large-scale and small-scale fading. Large-scale fading deals with spatial characteristics of the channels. Basic propagation models indicate that average received signal strength (RSS) power decreases logarithmically with distance. These models do not take into account the surrounding environment clutter that exists at different locations, such as buildings and tress. This leads to a variation of the measured signal about the mean of the predicted RSS at any particular distance between transmitter and receiver. This phenomenon is known as log-normal shadowing, and it is studied in more detail in Chapter 5. Small-scale fading, on the other hand, deals with both spatial

and temporal characteristics of the radio signal, and it describes the rapid fluctuations of the amplitude, phase, or multipath delays of the RSS over a short period of time or distance. This thesis deals exclusively with large-scale fading of the mobile radio propagation, and Chapter 3 describes how to remove small-scale fading effects from measured data.

1.4 Thesis Organization

Chapter 2 discusses and compares existing deterministic and empirical propagation models. Emphasis is placed on the empirical model. Chapter 3 describes how the experiment is setup and how data is manipulated to filter out small-scale fading. Chapter 4 describes the proposed model for the Tampa Bay area and shares the statistical analysis for each type of environment. Chapter 5 goes into the shadowing effect of the wireless channel in the Tampa Bay area and discusses the second order statistics of this effect; that is, the spatial correlation properties of shadowing effects. Chapter 6 revisits the contributions of this thesis and provides future study directions.

CHAPTER 2

PROPAGATION MODELS

Propagation models are mathematical tools used by engineers and scientists to design and optimize wireless network systems. The main goal in the design phase of the wireless network is to predict the probability of signal strength or coverage in a particular location, and avoid interference with neighboring sites. In the optimization phase the objective is to make sure the network operates as close as possible to the original design by making sure handoff points are close to prediction; coverage is within design guidelines such as in-door, in-car, and on-street RSS; and co-channel interference is low at neighboring sites. Also, in the optimization phase measured data collected from the live network may be used to tune the propagation models utilized in the design phase.

Although the propagation models used today have become more sophisticated due to computer advancement, these models are still very simplified versions of the complex characteristics of the electric and magnetic field in the real world. A complete characterization of the electric magnetic field would involve solving very complex equations such as Maxwell's Equations.

$$\boldsymbol{\Delta} \cdot \mathbf{E} = -\frac{\rho}{\varepsilon_0} \tag{1}$$

$$\boldsymbol{\Delta} \cdot \mathbf{B} = 0 \tag{2}$$

$$\boldsymbol{\Delta} \times \mathbf{E} = -\frac{\partial \mathbf{B}}{\partial t} \tag{3}$$

$$\boldsymbol{\Delta} \times \mathbf{B} = \mu_0 \mathbf{J} + \mu_0 \varepsilon_0 \frac{\partial \mathbf{E}}{\partial t} \tag{4}$$

The underlying problem would become even more complex when taking into consideration all existing propagation mechanisms such as reflection, diffraction, and scattering in a very dynamic environment such as a city. These mechanisms can vary significantly from the mean predicted RSS value at any point between transmitter and receiver. Some of theses variances are characterized by statistical distributions such as Rayleigh and log-normal. Consequently, due to the variance and unpredictability of the radio channel, it is not practical to use theoretical solutions to describe the radio channel but rather statistical methods.

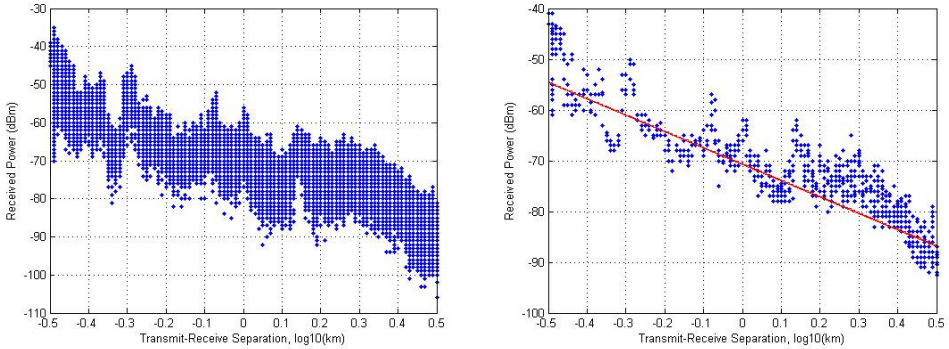

Figure 1. Sample of measured data with channel descriptions. On the left, all three phenomena of the channel description are inherited in data: path loss, shadowing, and small-scale fading. The plot on the right shows the data with small-scale fading removed.

Nonetheless, the current propagation models offer a very efficient and cost effective way for network planning. They are in fact derived from the equations of electromagnetic field theory. A summary of the derivation of these relations can be found in [1].

2.1 Introduction

There are two main types of propagation models: slope based and deterministic. Slope based models are based on empirical formulas, which themselves are based on measured data and the free space propagation model. The free space propagation model is used when line of sight between transmitter and receiver exists and can be represented by the Friss free space equation.

$$P_r(d) = \frac{P_t G_t G_r \lambda^2}{(4\pi)^2 d^2 L} \tag{5}$$

P_t is the transmitted power, $P_r(d)$ is the received power which is a function of the separation between the transmitter and receiver, G_t and G_r is the transmitter and receiver gain respectively, d is the distance separation between the transmitter and receiver in meters, L is system loss factor not related to propagation ($L \geq 1$), and λ is the wavelength in meters. More detailed information about this equation can be found in [1]

Deterministic models use ray-tracing techniques that rely on detailed terrain and clutter database to estimate diffraction calculation based on Huygen's principles of physical optics [2]. The prediction generated using deterministic models are very computer intensive. But new development in computer speed and algorithm as well as database accuracy has made deterministic models a good choice for propagation tools especially for in-building propagation design.

2.2 Comparison between Deterministic and Empirical Models

Understanding the limitations of various propagation models helps engineers achieve good engineering design. For this reason we will describe the most common models used today and then we will provide a brief comparison between deterministic and empirical path loss models.

2.2.1 Hata-Okumura Model

The most common used empirical model is the Hata-Okumura Model. Hata used predicted signal strength curves obtained by Okumura's data collection experiment throughout Japan to create some basic formulas [3]. These path loss formulas (in dB) were based on an urban free space propagation model, with correction factors to account for variation in other types of environment such as suburban, and open areas. The parameter for correction factors includes the base station and mobile antenna heights and center frequency.

$$L_p = 69.55 + 26.16 \log_{10} f_c - 13.82 \log_{10} h_b - a(h_m) + (44.9 - 6.55 \log_{10} h_b) \log_{10} R \qquad (6)$$

Where f_c is the frequency in MHz from 150MHz to 1500MHz, h_b is the effective transmitter antenna height in meters ranging from 30m to 200m. h_m is the effective mobile receiver antenna height in meters ranging from 1m to 10m. *R* is the distance between transmitter and receiver in km, and $a(h_m)$ is the correction factor for effective mobile antenna height, which is a function of the size of the coverage area. For a medium-to-small city the following correction factor is used.

$$a(h_m) = (1.1\log_{10} f_c - 0.7)h_m - (1.56\log_{10} f_c - 0.8) \tag{7}$$

For a large city the correction factors used are described below.

$$a(h_m) = 8.29(\log_{10} 1.54h_m)^2 - 1.1 \qquad f_c \le 300MHz \tag{8}$$

$$a(h_m) = 3.2(\log_{10} 11.75h_m)^2 - 4.97 \qquad f_c \ge 300MHz \tag{9}$$

To obtain the path loss for suburban area the following equation is used.

$$L_{ps} = L_p\{Urban\} - 2\log_{10}\left(\frac{f_c}{28}\right)^2 - 5.4 \tag{10}$$

And to obtain the path loss for an open area, the equation is below is used.

$$L_{po} = L_p\{Urban\} - 4.78\log_{10} f_c{}^2 + 18.33\log_{10} f_c - 40.94 \tag{11}$$

2.2.2 COST-231 Hata-Okumura Model

An extension to the Hata model described above is the COST-231 Hata model [1]. This model is designed to be used in the frequency band from 500 MHz to 2000MHz. As the Hata Model, the COST-231 is restricted to cell radius greater than 1 km and may not be suitable for cells on the order of 1km radius.

$$\begin{aligned} PL_{COST-231} &= 46.3 + 33.9\log_{10}(f_c) - 13.82\log_{10}(h_b) - a(h_m) \\ &+ (44.9 - 6.55\log_{10}(h_b))\log_{10} R + c_m \end{aligned} \tag{12}$$

For a large city the correction factor $a(h_m)$ is used below.

$$a(h_m) = 3.2(\log_{10} 11.75h_m)^2 - 4.97 \qquad f_c > 400MHz \tag{13}$$

For suburban or rural areas the correction factor $a(h_m)$ is used in the equation below.

$$a(h_m) = (1.1\log_{10} f_c - 0.7)h_m - (1.56\log_{10} f_c - 0.8) \tag{14}$$

As noted the $a(h_m)$ correction factors are the same for both the original Hata model as well as the COST-231.

2.2.3 SUI Model

Another model which is popular for broadband wireless communications is the Stanford University Interim (SUI) or Erceg model [4]. It has been accepted by the IEEE802.16 Broadband Wireless Access Working Group to evaluate fixed wireless applications air interface performance. The main difference from other models is that the path loss exponent is treated as a random variable in addition to the shadowing effects. The basic path loss equation for this model along with its correction factors are presented below.

$$PL = A + 10\gamma\log_{10}\left(\frac{d}{d_0}\right) + X_f + X_h + s \qquad d > d_0 \tag{15}$$

The other parameters are defined below.

$$A = 20\log_{10}\left(\frac{4\pi d_0}{\lambda}\right) \tag{16}$$

$$\gamma = a - bh_b + \frac{c}{h_b} \tag{17}$$

Here d is the distance between transmitter and receiver and d_0 is the reference distance at 100m from the transmitter. s is a log-normal distributed factor that is used to account for shadow fading. A is modeled as the free-space path loss formula and γ is the random variable path loss exponent that is dependent on the base station height h_b, and the environment category.

The environment categories with corresponding model parameter are shown in Table 1.

Table 1. SUI Models numerical values for different terrain (environment) categories.

Model Parameter	Terrain Category		
	A (Hilly/Moderate-to-Heavy Tree Density)	B (Hilly/Light Tree Density of Flat/Moderate-to-Heavy Tree Density)	C (Flat/Light Tree Density)
a	4.6	4.0	3.6
B (m^{-1})	0.0075	0.0065	0.005
c	12.6	17.1	20

Also, some correction factors for the operating frequency X_f and for the receiver height X_h are provided below.

$$X_f = 6.0 \log_{10}\left(\frac{f_c}{2000}\right) \tag{18}$$

For terrain category types A and B the following equation is used.

$$X_h = -10.8 \log_{10}\left(\frac{h_r}{2}\right) \tag{19}$$

For terrain category type C the following equation is used.

$$X_h = -20.0 \log_{10}\left(\frac{h_r}{2}\right) \tag{20}$$

2.2.4 CRC-Predict and Deterministic Models

Deterministic models are ray-tracing techniques based on geometric optics to estimate signal strength at any particular location. These techniques rely on detailed terrain and clutter databases to estimate diffraction calculations based on Huygen's principle of physical optics. A

program known as CRC-Predicit has been developed, for the most part, by the Communications Research Centre in Ottawa, Canada [2]. This program is based on several parameters characterizing the local environment of the mobile antenna. It numerically solves the integral for Huygen's principle and the field can be calculated using the equation below.

$$E(x_2, z_2) = \sqrt{\frac{kx_1}{2\pi i(x_2 - x_1)}} \times \left[\int_{h_1}^{\infty} E(x_1, z_1) e^{ikr} dz_1 + \int_{h_1}^{\infty} E(x_1, z_1) e^{ikr_R} dz_1 \right] \tag{21}$$

Here $k = \frac{2\pi}{\lambda}$ is the propagation constant, r is the distance from (x_1,z_1) to (x_2,z_2), r_R is the length of the reflected path, and R is he reflection coefficient of the ground.

The accuracy of ray tracing in predicting signal strength has been increased by the growth in computational capabilities and database storage.

2.2.5 Model Comparisons

In [5], the author provides a comparison between deterministic and empirical models. The deterministic models show a difference of 0.75dB and 1.46dB between two popular empirical modes, but a difference of 12.6dB when compared against the Hata model. This seems to agree with our analysis since the Hata model analysis herein provides a pessimist prediction of the path loss as seen in Figure 2. This difference is due to the more simplistic approach of the Hata model, which accounts for only three correction factors and excludes terrain profile and clutter absorption losses. The most common way of predicting diffraction losses caused by terrain and buildings is the use of the Knife-edge diffraction model. In this model the losses caused by obstructions are estimated by the using Fresnel Zone Geometry solutions. A detailed analysis on this model is presented in [6]. It is worth mentioning that diffraction models are also incorporated along with terrain and clutter databases, in tools that support empirical models.

Figure 2 shows the path loss for comparison for different empirical models. No deterministic model is shown on the plot. The reason being is threefold. First, this thesis focuses on empirically formulated models only. Secondly, deterministic models require terrain and

clutter database in order to make a fair comparison. Finally, the lack of access to any specific deterministic tool would make fair comparisons very difficult. The mathematical code for these tools is usually closely guarded and an attempt to simulate the deterministic model using a programming language would be impractical.

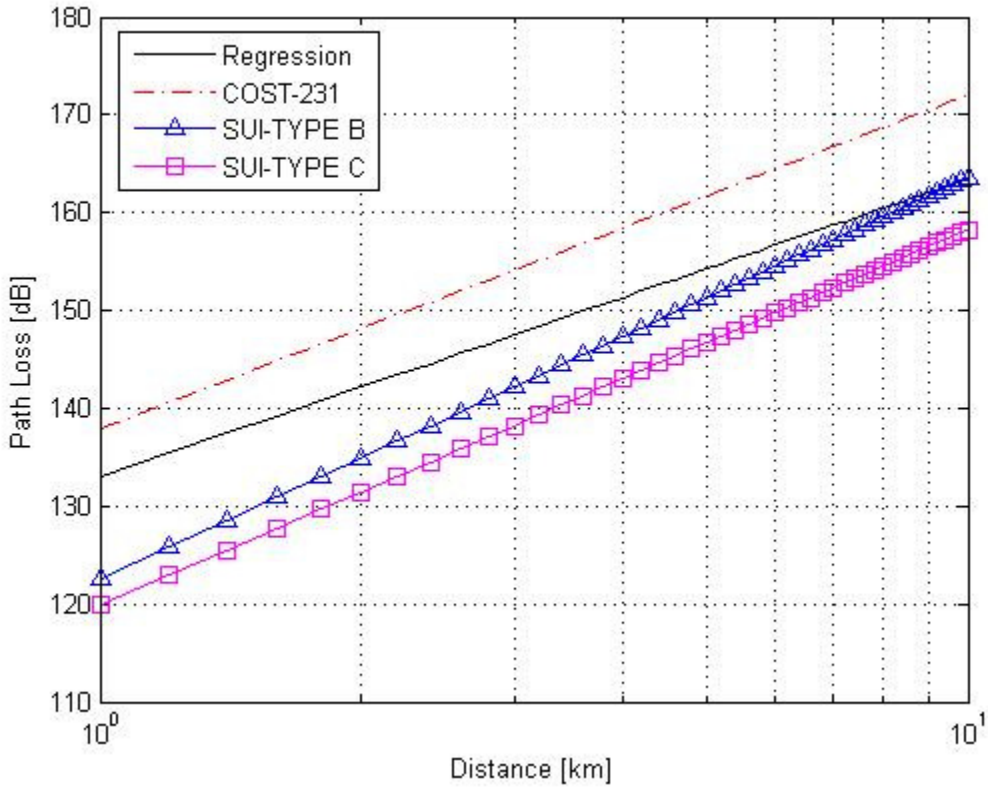

Figure 2. Empirical models are compared against the regression analysis of the measured data.

The deterministic model, at first, seems to be a more accurate way of estimating signal strengths. However, the slope model it is still being widely used today. For instance, the SUI model is recommended by the IEEE 802.16 Broadband Wireless Access Working Group as the channel model choice for fixed wireless applications. Furthermore, empirical models have become more accurate as parameter correction factors are discovered and terrain and clutter databases are integrated in these models. An assumption may then be made that the deterministic approach is more appropriate to an indoor environment, and that the slope model is more appropriate for outdoor environment propagation planning. In order for any model to offer a

complete picture of the propagation characteristics of specific technologies being deployed, all possible parameters such as the frequency and environment types of the Tampa Bay area must be studied in detail. For instance, the extended version of the Okumura-Hata model, namely COST-231, does not support frequencies beyond 2MHz, and the SUI models do not have a profile for urban environment. By the same token, it is impractical to collect data that is capable of covering all the possible parameters and environments. It is feasible, however, to build upon existing models of the unique characteristics of the environment being studied, in this case the Tampa Bay area.

Table 2. Comparison between different models against measured data.

	COST 231			SUI TYPE B			SUI TYPE C		
SITE	mean err	std dev err	RMSE	mean err	std dev err	RMSE	mean err	std dev err	RMSE
A	3.3462	0.0389	3.3465	-6.9102	2.0115	7.1909	-11.379	1.2966	11.451
B	5.5045	0.5736	5.5336	-6.079	0.9863	6.1568	-10.4785	0.2825	10.4823
C	-0.38	1.588	1.616	-10.4403	3.6188	11.0368	-14.8921	2.9066	15.1671
D	10.2085	1.2989	10.2891	-1.2013	2.9136	3.1221	-5.6305	2.205	6.0381
E	8.0727	0.6495	8.0982	-2.2766	2.5946	3.4306	-6.7514	1.8788	7.0025
F	10.5181	2.9324	10.9107	0.7979	5.0601	5.068	-3.6134	4.3544	5.6219
G	5.2511	0.4013	5.266	-6.1576	1.2133	6.2734	-10.5868	0.5047	10.5985
H	2.5992	0.0493	2.5996	-8.0016	1.8189	8.2013	-12.4858	1.1015	12.5332
I	8.3485	2.6434	8.7484	-1.7118	4.6741	4.9298	-6.1636	3.962	7.3038
J	6.9968	2.3194	7.3633	-3.604	4.1876	5.4903	-8.0881	3.4702	8.7863
K	4.3706	1.2347	4.538	-5.6886	0.796	5.7428	-10.1403	0.0838	10.1407
L	7.9327	1.2791	8.0329	-3.1011	3.012	4.3002	-7.5729	2.2966	7.9062
M	1.522	1.9936	2.4909	-9.7661	0.341	9.7719	-14.2122	1.0523	14.2502
N	8.6755	0.6072	8.6962	-1.0459	2.7349	2.9002	-5.4572	2.0292	5.8146
O	4.3457	0.9143	4.4388	-2.1644	3.8237	4.3575	-5.9283	3.2216	6.7304
P	3.788	3.7754	5.3191	-5.3674	1.494	5.5671	-9.6889	2.1853	9.9271
Q	-3.1416	1.4733	3.4631	-13.7435	0.3949	13.7491	-18.2277	0.3225	18.2305
R	-5.36	0.4218	5.3763	-14.1631	2.7945	14.4302	-18.4192	2.1136	18.5375
S	-2.2462	0.6442	2.3349	-13.7733	2.222	13.9475	-18.1832	1.5165	18.245
T	16.1922	1.8484	16.2951	7.5896	0.5745	7.6108	3.3725	0.1001	3.3739
U	16.3712	3.197	16.6737	7.5935	5.5696	9.3812	3.3373	4.8888	5.8752
V	16.0089	3.3787	16.3539	7.4063	5.8016	9.3691	3.1892	5.1269	5.9904
W	14.3483	0.7695	14.3685	5.1941	1.5119	5.405	0.8726	0.8206	1.1917
X	7.3683	0.9746	7.4311	-3.2863	2.8187	4.3095	-7.771	2.1013	8.0441
Y	8.2724	2.2216	8.5593	-2.0768	4.1667	4.6149	-6.5517	3.4509	7.3874
Z	10.6449	2.7822	10.9948	0.6911	4.8439	4.8405	-3.7493	4.1335	5.5473
AA	4.8836	1.7739	5.1892	-3.7202	4.1968	5.5741	-7.9373	3.5222	8.6681
BB	5.4894	2.2952	5.9403	-4.232	0.1675	4.2352	-8.6433	0.8732	8.6864
CC	6.8055	0.008	6.8055	-1.7983	2.4149	2.9898	-6.0154	1.7403	6.2568

Table 2 shows how the different models fit the measured data. RMSE values for the COST-231 model ranged from 1.6dB to 16dB; values for SUI Type B ranged from 2.9dB to 14.4dB; and values for SUI-C ranged from 1.2dB to 18.5dB. Positive values for mean error indicate the model is pessimistic, i.e., the path loss prediction is higher then expected. Negative

values indicate the path loss prediction is lower then expected. Sites Q, R, and S shows a much higher error rate than the others. This is because these sites are located around bridges. A more detailed explanation is discussed in Chapter 5. Overall, SUI Type B model shows a better fit mainly because this model was created to support broadband wireless applications with parameters closer to the data used for this thesis.

CHAPTER 3

EXPERIMENT

A crucial part of any experiment study is to make sure the data collected is consistent throughout the experiment. In order to extract the intended information about the environment, a systematic procedure has to be put in place prior to the collection of data. During the measurement campaign, the equipment was calibrated and baseline measurements were taken before each data collection. This procedure included a complete log of all information pertaining to site location and equipment type. Gains and losses about the antennas and cables were noted to effectively calculate the path loss of the propagation model. In addition, it was important to take pictures of the surrounding environment. These pictures can help in determine anomalies in the data and validate clutter and terrain databases. In this chapter experiment equipment setup and collected data pre-processing analyses are discussed.

3.1 Tampa Bay Environment

In the summer of 2007, RSS data was colleted from 29 locations around the Tampa Bay area. The structure of the 29 sites consisted of existing locations - towers and rooftops - as well as crane mounts as seen in Figure 3. The antenna heights were in the range of 20m to 58m.

Figure 3. One of the crane mounts setup with transmitter for data collection.

The sites were located throughout the Tampa Bay area which encompasses of metropolitan areas of Tampa, Clearwater, and St. Petersburg. The areas consist of flat terrain with dense residential zones, heavy vegetation, and business districts with tall buildings. Three major bridges spanning over 10km link the major metropolitan areas, making these routes very important for both commercial and public needs. These bridges are also vital routes for emergency evacuations. Figure 4 depicts one of the unique characteristics of the Tampa Bay area, Clearwater Beach, which is a populated patch of land in between the main coastal areas and a harbor along the Gulf of Mexico. This type of environment is very challenging for planning proper coverage and mitigating the Radio Frequency (RF) energy interference created by transmitters near the water.

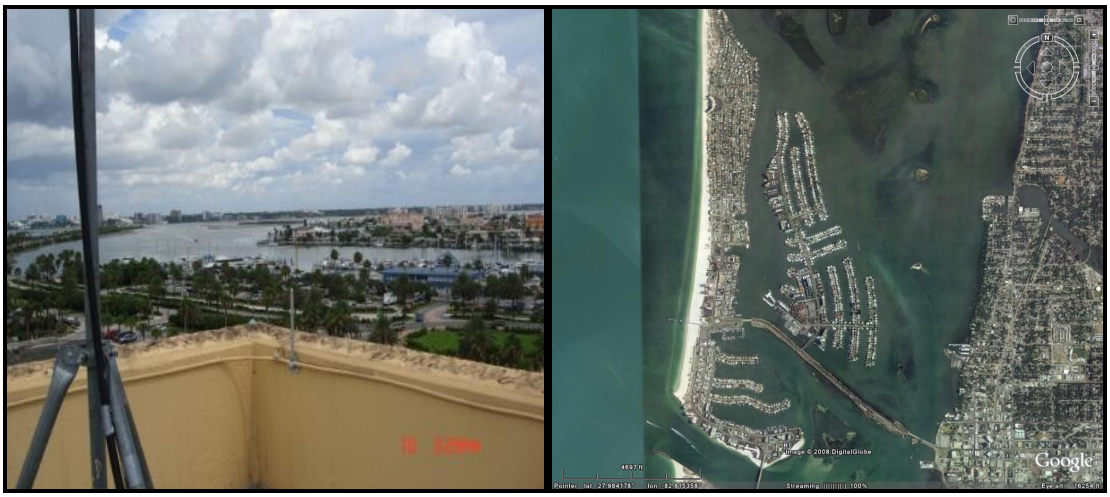

Figure 4. The Tampa Bay area offers very unique characteristics such as coastal areas.

Although Tampa Bay's downtown areas, are relatively small compared to other major metropolitan areas in the U.S., downtown Tampa has high rises typical of heavy urban environments as shown in Figure 5.

Figure 5. Building layout of downtown Tampa.

Suburban areas in the Tampa Bay area are similar to those encountered throughout the U.S. which is composed of flat terrain and semi-dense tree distribution. These areas usually contains single story homes as shown in Figure 6.

Figure 6. Typical Tampa Bay suburban area.

One of the main motivations to study the Tampa Bay area was the number of bridges that link the cities such as those shown in Figure 7. Bridges are of major importance due to Tampa Bay's heavy traffic volume during business hours. Therefore an adequate quality of service around the bridges is critical.

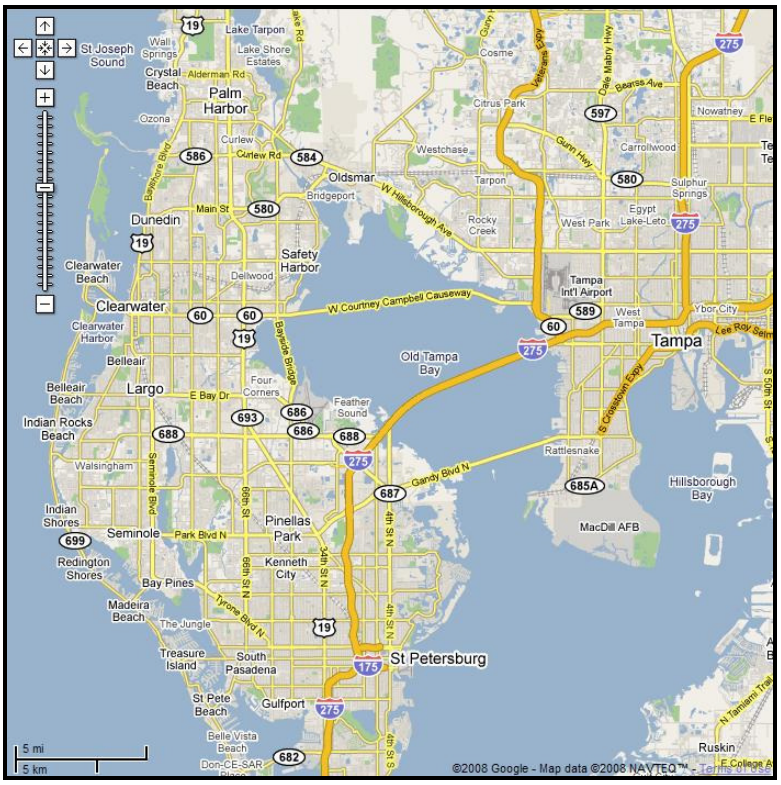

Figure 7. Bridges link major metropolitan areas in the Tampa Bay area. It includes the cities of Clearwater, Tampa, and St. Petersburg.

Commercial areas around the Tampa Bay area are composed of wide streets and one to two story business units similar to the one in Figure 8. These environments are the most inclined to have tunnel effects, therefore the need to carefully filter the data prior to analyzing it. Tunnel effect occurs when RSS is channeled by the buildings so that the strongest paths are not necessarily the direct paths diffracted over the edge of nearby obstructing buildings, but are found to be from directions parallel to the streets [7].

Figure 8. Typical commercial area in Tampa Bay area.

The Tampa Bay area has a population of about 2.5 million people, which makes an attractive metropolitan area to deploy new networks and services. This area also has unique and diverse environments that can be a challenge to plan for new networks. The surrounding bodies of water make it hard to contain the RF energy and prevent interference. One of the goals of this thesis is to provide a more optimized model to help mitigate interference and provide a better quality of service around this area.

3.2 Equipment Setup

The base stations transmitted a continuous wave (CW) signal, with an omni-directional antenna with maximum gain of 8.5 dBi, from a 20 W transmitter close to 2.6 GHz. An example of a typical equipment setup is shown in Figure 9. Here the equipment is located on a rooftop somewhere in the Tampa Bay area. The receiver antenna was placed on a vehicle about 2 m above the ground. The vehicle was driven around the area.

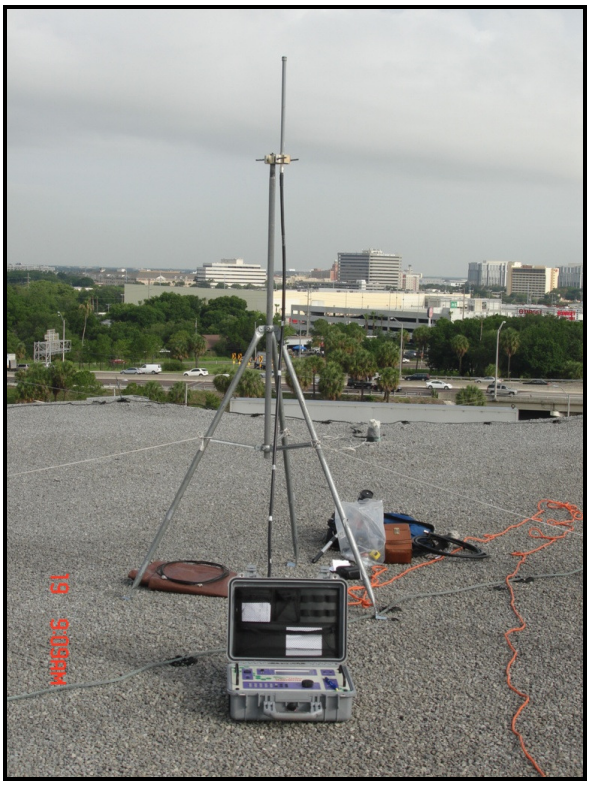

Figure 9. Typical transmitter setup.

The transmitter equipment used was a Gator Class A transmitter with maximum output power of 20 W and frequency range of 2.5 GHz to 2.7 GHz. The receiver equipment consisted of a Coyote dual modular receiver which was integrated with commercial software to map the RSS values with GPS information. The test equipment is shown in Figure 10.

Figure 10. The transmitter was calibrated and values were logged prior to data collection.

For every base station experiment a checklist was logged with detailed procedures and values such as transmitted power, cable power losses, and center frequencies. These values were used at a later time for link budget purposes. These procedures were kept consistent throughout the campaign measurement.

As indicated in Chapter 1, there are two major types of fading in the mobile wireless environment, large-scale and small-scale. Although the receiver equipment used was capable of averaging out the small-scale phenomena in real time, this was not the case in this experiment. Therefore the averaging had to be completed after the data was collected. The next section provides the methods used to remove small-scale fading from the measured data.

3.3 Rayleigh Fading

In order to estimate the local mean received power of the path loss, the small-scale fading characteristics of the radio signal had to be removed. The first rule is to determine the proper distance interval that will preserve path loss and shadowing effects statistics. The length of a local mean has to be chosen properly. That is, if the length is too short, the fast fading is still present after the averaging process. If the length is too long, shadowing effects are removed.

Small-scale fading can be modeled by Rayleigh distribution assuming the signal has no line of sight (LOS). The measured length of a mobile radio signal necessary to obtain the local mean of the path loss power has been determined to be in the range of 20 to 40 wavelengths. A detailed derivation of this process can be found in this reference [8]. Over 3 million data points in different locations for each transmitter station were measured in this experiment. A length of 40 wavelengths was used to obtain the local mean as suggested in [8]. This implies a typical range of standard deviation of 0.06 and a spread of 1 dB. Since the frequency used was 2.6 GHz, the length of 4.5 m was used to obtain the local mean.

In Figure 11 a small segment of the raw collected data is shown to illustrate how a very small sample of data needs to be filtered in order to extract the corrected statistical parameters of interest.

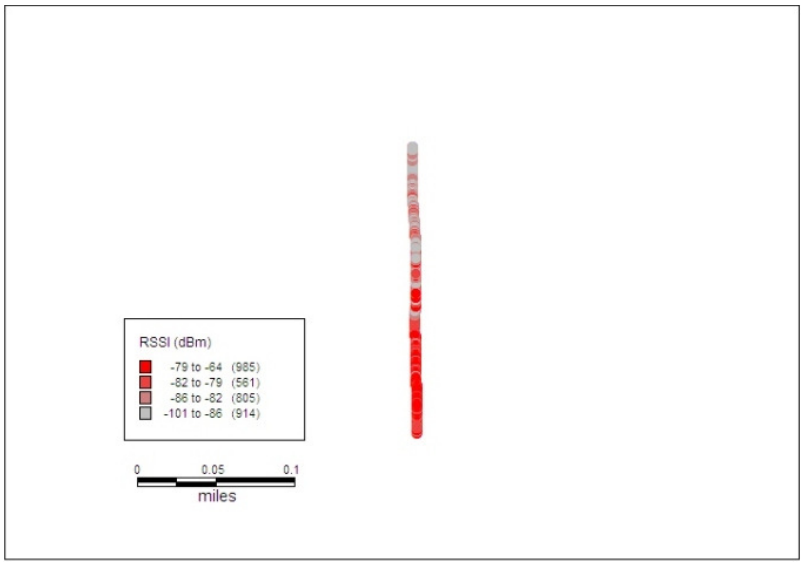

Figure 11. Sample length of data to be filtered.

As seen from Figure 12, the dynamic range from the sample data is about 20 dB in a very short segment of the data.

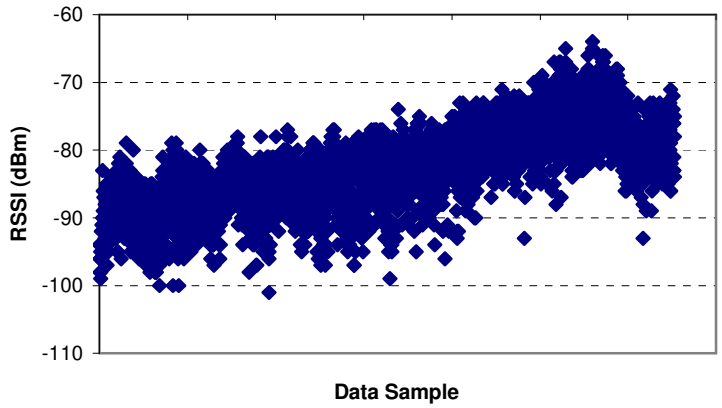

Figure 12. Sample unfiltered data.

After the data is filtered as illustrated in Figure 13 the dynamic range is less then 5 dB; small-scale fading is removed and the path loss and shadowing (variance) effects of the data are preserved.

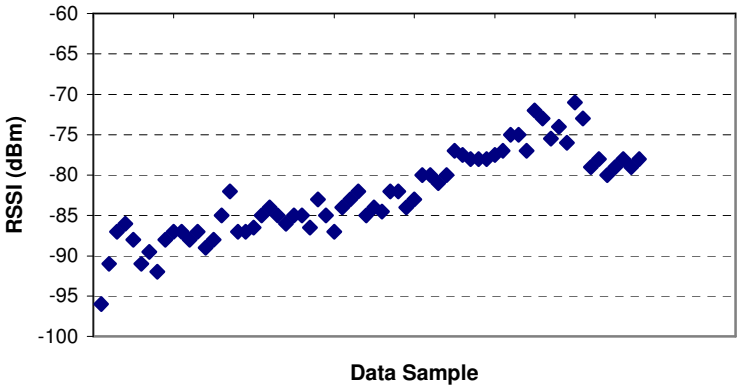

Figure 13. Sample filtered data.

Figure 14 is shown to illustrate the statistical time varying nature of the received signal which once more shows Rayleigh distribution characteristics.

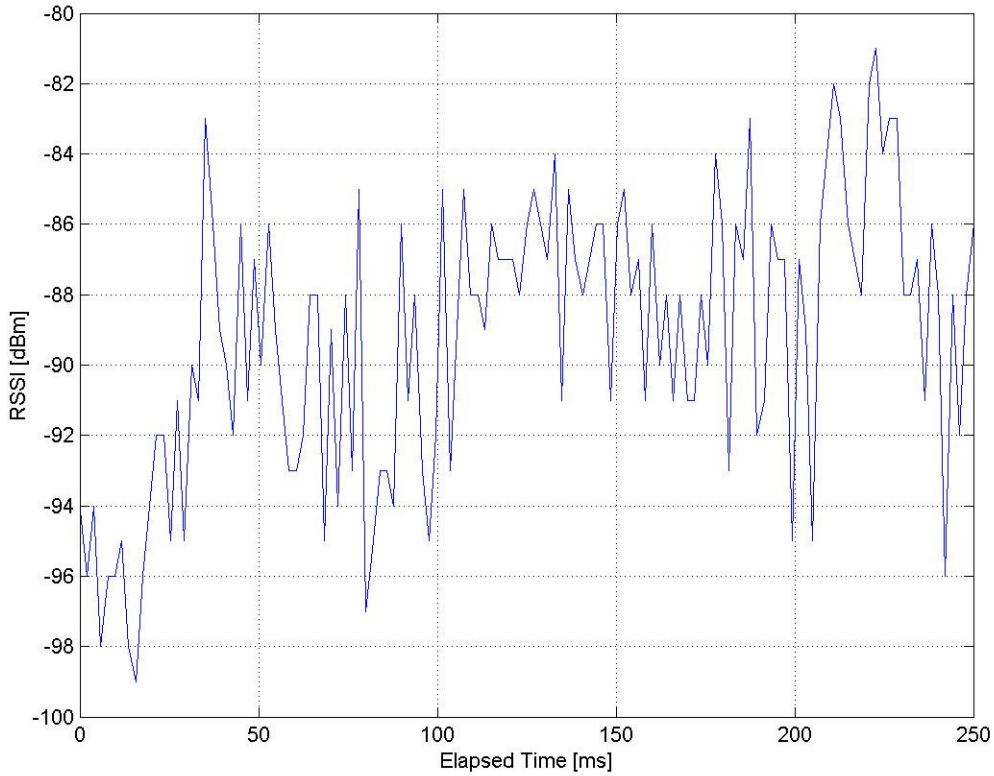

Figure 14. A small sample of the data showing Rayleigh fading characteristics.

Since short-term fading deals mainly with the relationship between the time rate of change in the channel and the transmitted signal, it is noteworthy to illustrate the received signal as a function of time shown in Figure 14. Please note that a more accurate description of the short-term fading in this signal should not include values approximately between 0 to 50 milliseconds since it clearly shows the signal experiencing shadowing effects or other phenomena that can not be described by Rayleigh distribution.

CHAPTER 4

ADAPTED MODELS FOR TAMPA BAY AREA

The main objective of this campaign was to collect RSS data throughout the Tampa Bay are and optimize the existing models. This task is known in the industry as "model tuning" or "propagation model optimization". For the 2.6 GHz band channel, the COST-231 Hata model and Stanford University Interim (SUI) models were used to compare against the measured data. Again, we are not going to use deterministic models for reasons explained in Chapter 2. Existing models such as SUI and COST-231 Hata model are based on data collected in different areas, and may not fit every possible morphology type. For instance, the SUI method is based on experimental data collected in several suburban areas in New Jersey and around Seattle, Chicago, Atlanta, and Dallas. None of those areas have characteristics that resemble the Tampa Bay area. The Hata Model is based on data collected in Japan by Okumura. Moreover, urban areas such as Tokyo are very dissimilar to the urban areas around the Tampa Bay area. Downtown Tokyo extends its high rise buildings for several kilometers whereas downtown Tampa consists of tall buildings only within a radius of two kilometers. Therefore, the motivation of this chapter is to provide an adapted model that better describes the propagation characteristics in the Tampa Bay area. The first adapted model is based on a two-slope based empirical model that is to be used for bridges in the Tampa Bay area. The second adapted model is based on regression analysis for the area's suburban environments. The third adapted model is also based on regression analysis but uses a much shorter distance for the slope intercept to account for the urban environment.

4.1 Introduction

The adapted model proposed here is based on least square regression analysis. We first classify the different types of terrain, and then sub-categorize based on specific characteristics. The major terrain categories are urban, suburban, and rural. Furthermore, we subcategorize the suburban areas as follows: residential only with trees, residential/industrial with trees, bridges and coastal. For the bridges, a two-slope method is used to provide a better fit than existing models. The two-slope method is used in microcellular design, but it can also be used for bridges and highways. In [9] it is suggested that a two-slope method be used to provide a more accurate model particularly for a more efficient system design employing less base stations to achieve the same quality of service.

The first step in the process is to average out fast fading (Rayleigh fading), described in detail in Chapter 3. This is done in order to obtain the local average power, or local mean. The measured spatial length of the RSSI values to obtain the local average was determined to be in the range of 20 to 40 wavelengths, as described in Section 3.2. In this case for a center frequency of 2.6 GHz, the data is averaged approximately for a distance segment of 4.5 m. Fast-fading is due to multipath effects caused by reflections. Direct lines of sight are superimposed on slow and long term fading signals which are caused by diffraction and distance respectively.

The second step was to calculate the path loss exponent of each site. For this a linear regression using least square was applied to each site. The next section gives an overview of the regression analysis that will be used to develop the adapted models.

4.2 Regression Analysis

More in depth material about this section is obtained from [10], which proved to be a great resource in understanding the material herein.

Regression analysis is used to relate variable dependence on another. In the specific case of propagation analysis, it helps to explain the RSS dependence as a function of the logarithmic distance between the transmitter and receiver, as illustrated in Figure 15.

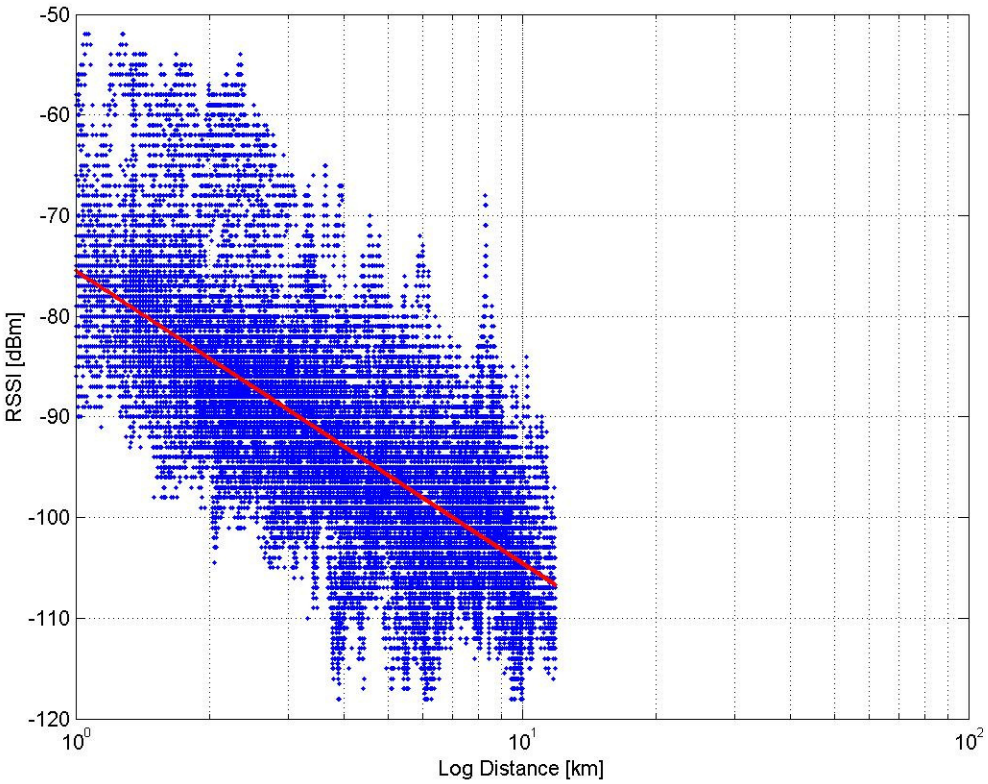

Figure 15. Typical scatter plot for a transmitter located in a suburban environment. The red line is the corresponding least-square linear regression fit.

Using Y_i to denote the RSS values in dBm, and X_i to indicate the RSS value corresponding distance in logarithmic scale, we can specify that on the average shown below.

$$\hat{Y}_i = a + bX_i \tag{22}$$

Where a is the intercept and be b the slope (i.e., the path loss exponent). Parameter extracted from the analysis such as the path loss exponent and intercept can then be used to make relations between different environments and site configurations. The least-square method is the

most common procedure in computing these parameters. The least-square method involves choosing *a* and *b* from Equation (21) so that the sum of the squared deviation is minimized.

$$\sum_{i=1}^{n}\left(Y_i - \widehat{Y}_i\right)^2 \tag{23}$$

The parameters *a* and *b* can be obtained using the formula below and the derivation can be found in [10].

$$b = \frac{\sum X_i Y_i - \frac{\sum X_i Y_i}{n}}{\sum X_i^2 - \frac{\left(\sum X_i\right)^2}{n}} \tag{24}$$

$$a = \overline{Y} - b\overline{X} \tag{25}$$

The derivation of the formulas above requires solving partial derivatives and different algorithms may be used to compute these values. For this thesis the MATLAB function "polyfit" was used to compute coefficients *a* and *b*.

4.3 Statistical Parameters for Goodness of Fit of Regression Analysis

The most common way of determining how a model fits against the measured data is to use root mean square error (RMSE) calculations, and R^2 which is referred as the *coefficient of determination*. These tests compute the amount of variation that is left over from the distance dependence variation (in path loss case), from the least square fit and the degree of linear association between the variables. R^2 is obtained by taking the ratio of the explained variation over the total variation. The largest possible value is $R^2 = 1$, and the smallest is $R^2 = 0$. These indicated perfect fit and complete lack of fit respectively.

$$R^2 = \frac{\sum (\widehat{Y}_i - \overline{Y})^2}{\sum (Y_i - \overline{Y})^2} \tag{26}$$

Where Y_i is the measured RSS value, $\overline{Y}$ is the sample mean measured RSS value, and $\widehat{Y}$ is the RSS predicted value of the least square fit of the regression analysis.

RMSE is also known as Root Average Squared Prediction Error (RASPE). It gives a summary of the analyzed data in the units of the dependent variable, which in this case is the RSS in dB units.

$$RMSE = \sqrt{\frac{\sum_{j=1}^{n}\left(Y_j - \widehat{Y}_j\right)^2}{n}} \tag{27}$$

A RMSE value closer to 0 indicates a better fit. However, the performance of model is deemed acceptable if it provides an overall RMSE of about 6-7 dB as stated in [11].

4.4 Results

The parameters obtained from the regression analysis are discussed in this section. First, the general results for all sites are briefly discussed. We then classify different environments and adapt the log-distance path loss model to account for the statistics of the specific areas. More specifically we discuss the propagation characteristics of bridges, suburban, and urban environments in the Tampa Bay area.

4.4.1 General Results

The results presented here show all the parameters for the sites where data was collected. These results have been obtained through regression analysis using least-square methods and compared against the different models as shown in Table 3. Please note that the regression analysis is assumed to have zero mean error when compared with the models in Chapter 2.
The results presented here show the statistical analysis of sites located in particular environments or morphologies. Table 3 shows the path loss exponent, RSS intercept, along with the height of the sites.

Table 3. Site antenna heights and model parameters.

SITE	ANT Height (m)	Morphology	Path Loss Exponent	RSSI Intercept (1 km)	Comments
SITE A	**20**	Suburban	3.30	-90.08	Flat Terrain/Trees/Houses/Coastal
SITE B	**27**	Suburban	2.29	-82.13	Flat Terrain/Trees/House/Industrial/Coastal/Bridges
SITE D	**27**	Suburban	3.56	-84.03	Flat Terrain/Heavy Trees/Industrial/Highways/Major Roads
SITE E	**27**	Suburban	4.24	-68.90	Flat Terrain/Highway/Bridges/Coastal
SITE F	**28**	Suburban	2.35	-81.47	Flat Terrain/Trees/House/Bridges/Coastal/Major Roads
SITE G	**28**	Suburban	3.38	-96.34	Flat Terrain/Trees/Industrial/Major Roads
SITE H	**30**	Suburban	3.81	-72.73	Flat Terrain / Heavy Trees /Houses/ Industrial / Coastal / Bridges
SITE I	**30**	Suburban	4.93	-76.42	Flat Terrain/Condominiums/Coastal
SITE J	**34**	Suburban	2.39	-85.12	Flat Terrain/Heavy Trees/House/Industrial/Major Roads
SITE K	**34**	Suburban	4.34	-77.49	Flat Terrain/Heavy Trees/Industrial/Airport/Major Roads
SITE L	**34**	Suburban	3.26	-81.60	Flat Terrain/Condominiums/Coastal
SITE N	**37**	Suburban	2.48	-86.17	Flat Terrain/ Hearvy Trees/ Houses/ Industrial
SITE O	**37**	Suburban	3.92	-80.53	Flat Terrain/ Heavy Trees/Houses/Industrial/Highway
SITE P	**37**	Suburban	2.87	-92.49	Flat Terrain/Heavy Trees/House/Industrial/Major Roads
SITE Q	**39**	Suburban	3.43	-84.19	Flat Terrain/Heavy Trees/House
SITE R	**40**	Suburban	3.20	-81.34	Flat Terrain/Heavy Trees/House/Industrial/Major Roads
SITE T	**43**	Suburban	2.55	-85.69	Flat Terrain/Heavy Trees/House/Industrial/Major Roads
SITE U	**43**	Suburban	3.44	-84.25	Flat Terrain/Heavy Trees/Major Roads
SITE V	**43**	Suburban	3.97	-86.91	Flat Terrain / Heavy Trees / Heavy Houses / Coastal
SITE W	**44**	Suburban	3.05	-81.25	Flat Terrain/Heavy Trees/Coastal
SITE X	**49**	Suburban	2.90	-81.47	Flat Terrain/Heavy Trees/Houses/Industrial/Major Roads
SITE Y	**53**	Suburban	4.11	-78.95	Flat Terrain/Heavy Trees/House/Highway
SITE Z	**55**	Suburban	2.86	-78.92	Flat Terrain / Heavy Trees / Heavy Houses
SITE AA	**55**	Suburban	3.50	-79.11	Flat Terrain/Heavy Trees/House
SITE AB	**57**	Suburban	3.10	-89.64	Flat Terrain/Trees/Houses
SITE AC	**58**	Suburban	3.55	-78.11	Flat Terrain/ Heavy Trees/Houses/Major Roads
SITE C	**27**	Urban	2.89	-89.61	Flat Terrain/Tall Buildings/Coastal
SITE M	**36**	Urban	2.43	-84.76	Flat Terrain/Tall Buildings/Industrial
SITE S	**40**	Urban	2.61	-85.09	Flat Terrrain/Tall Buildings

The antenna height ranged from 20-58 m. The path loss exponent for suburban areas ranged from 2.29 to 4.93. An attempt was made to validate the findings of [4] where evidence is shown that the path loss exponent is strongly dependent on the base station antenna height. Unfortunately, we only had sites with antenna heights ranging from 20-58 m, whereas in [4] the heights ranged from 10-80 m. This made it very difficult to draw any conclusions as shown in Figure 16.

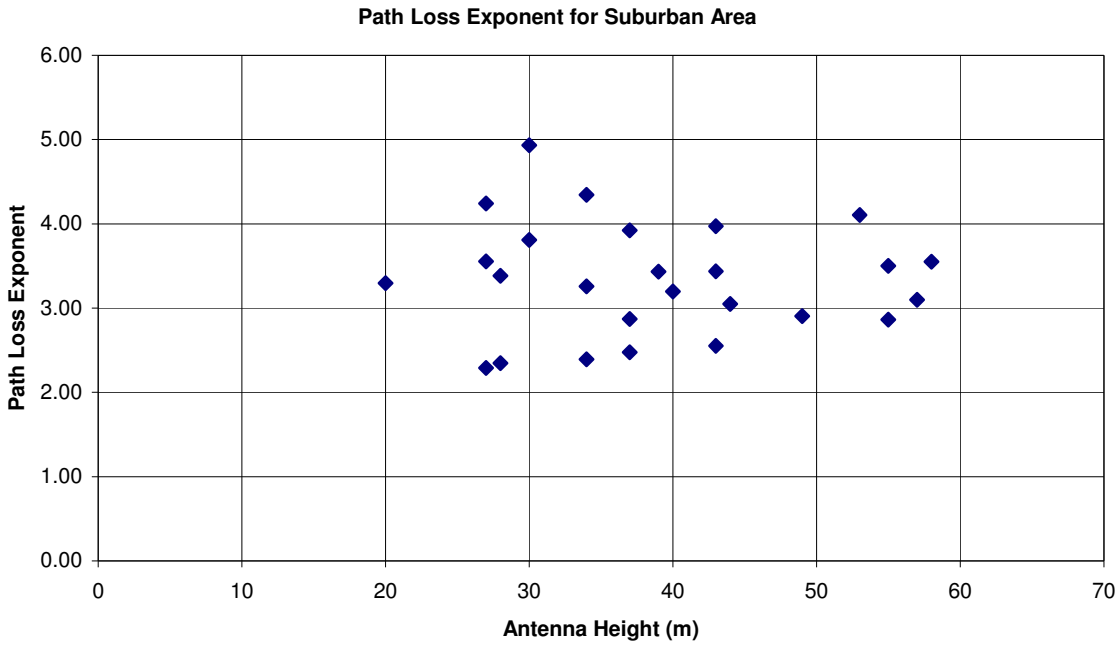

Figure 16. Path loss exponent as a function of antenna height for suburban area.

Since the data collected was from an omni-directional transmitter, the possibility of the signal strength serving different environments was very common. In addition to filtering the data as discussed in Chapter 3, we had to filter the data to make sure the area being studied was not contaminated by too may types of environment. This approach emphasizes the need to proper ly filter the data before to start analyzing it or making any conclusions. The remanding subsections discuss the specific environments and adapted models developed in this thesis.

4.4.2 Bridge Analysis and Model for Tampa Bay

Some two-slope models have been used to predict coverage in highways [9] but, a specific model in the literature has not been proposed for bridges. This is particularly important to the Tampa Bay area since bridges in this area are the major commuter routes among the cities as mentioned in Chapter 3. Also, in an emergency situation these bridges are major routes of evacuation, so it is paramount that propagation of radio link is well understood in these areas.

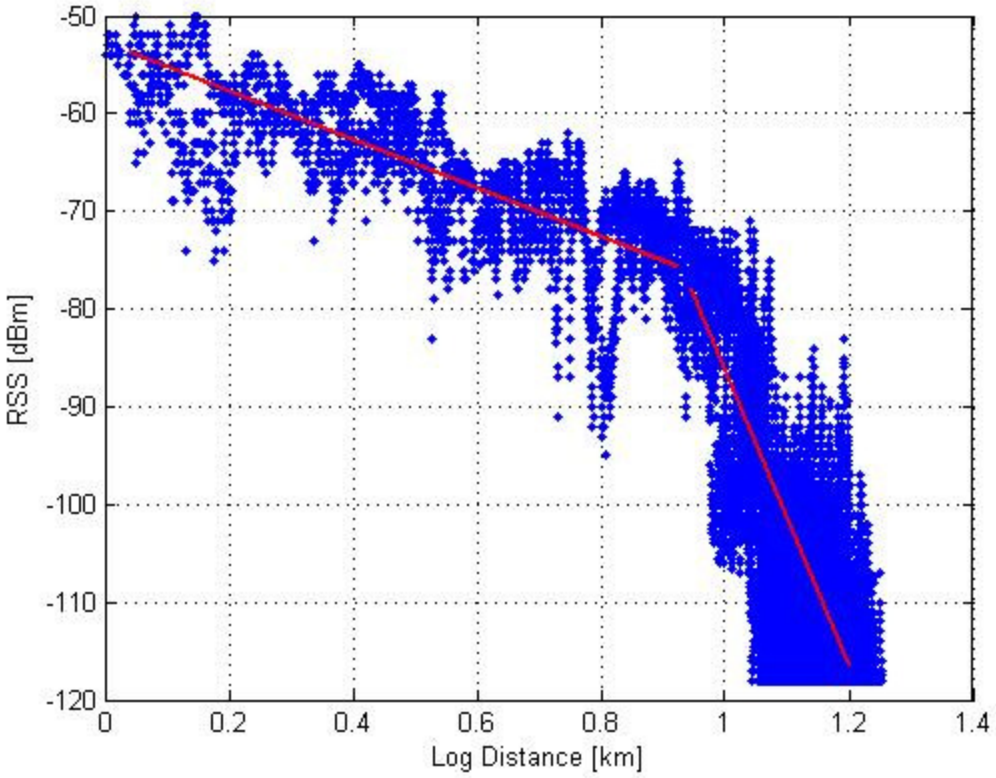

Figure 17. Data from a cell serving a major bridge in the Tampa Bay area. The straight lines represents the slope for two different segments where the break point is approximately the length of the bridge.

Assuming we use the free space loss equation for the reference distance, i.e.

$$PL_o = 20\log_{10}\left(\frac{4\pi d_o}{\lambda}\right) \tag{28}$$

Then, we can derive the formula below.

$$PL_{Bridges\_Tampa} = \begin{cases} PL_0 + 27.0\log_{10}(d) & d < d_{BP} \\ PL(d_{BP}) + 75.0\log_{10}(d) & d \geq d_{BP} \end{cases} \tag{29}$$

The piecewise equation below can be used to determine the path loss before and after and break point distance d_{BP}.

As can be seen from the results below, when the two-slope method is applied to a site serving the three major bridges in Tampa Bay a better fit is achieved. The main parameter to this model is the length of the bridge itself.

Table 4. One-slope vs. two-slope parameters.

SITE A				
		Path Loss Exponent	***RMSE***	***R^2***
One Slope	**s**	7.30	8.75	0.70
Two Slope	**s1**	2.30	3.88	0.71
	s2	8.80	6.87	0.37

SITE C				
		Path Loss Exponent	***RMSE***	***R^2***
One Slope	**s**	5.20	8.13	0.49
Two Slope	**s1**	3.08	4.49	0.73
	s2	3.10	7.15	0.07

SITE D				
		Path Loss Exponent	***RMSE***	***R^2***
One Slope	**s**	6.30	9.80	0.65
Two Slope	**s1**	3.10	5.11	0.74
	s2	6.20	9.02	0.16

The results shown in Table 4 indicate that the first slope, which is calculated from the reference distance of one mile to the break point distance. The break point distance is approximately the distance of the bridge, and the slope for distance decays much slower than the second slope. This can be explained by the near line of sight that is caused by the elevation of the bridges and the attenuation caused by the water which is much lower than in land. The second slope decays much faster and further analysis is recommended to explain the low coefficient of the determination.

4.4.3 Suburban Environment Analysis and Model for Tampa Bay Area

The initial results showed that further analysis needed to be performed. The data was filtered based on specific locations under the same type of environment. If the majority of the data was collected in a suburban environment, it is possible that a significant number of data points can be located in an urban or rural environment. This can contaminate the data and skew the main parameters of interest. For instance, Site I showed a path loss exponent value of 4.93.

Further investigation of this site shows it is located in a coastal area and it is surrounded by high rise condominiums. After filtering the data the values become less spread out.

The values for six suburban sites located in the same environment are shown in the tables below. As noted, the path loss exponents are within very close range.

Table 5. Path loss exponent and intercept for five suburban sites.

SITE	PathLoss Exponent	Path Loss 1km (intercept)
A	3.20	132.14
B	2.86	129.72
C	2.97	129.54
D	2.90	132.64
E	3.20	129.58

Table 6. Mean average of path loss exponent and 1 km intercept for suburban sites.

Suburban Tampa	
PathLoss Exponent Mean Average	**Path Loss 1km (intercept) Mean Average**
3.02	131.72

$$PL_{Sub\_Tampa} = 131.72 + 30.2\log(d) \tag{30}$$

Table 7. RMSE comparison between models.

	RMSE		
SITE	**TAMPA BAY**	**COST-231**	**SUI TYPE B**
A	1.30	8.13	3.32
B	1.76	10.36	3.01
C	1.58	10.94	4.92
C	0.57	8.12	4.16
E	1.02	8.76	4.74

The results in Table 7 show very good agreements with the adapted Tampa Bay model with a very close RMSE range between 0.57-2.18 dB. As expected, the COST-231 model did not show a good fit to the data. The SUI Type B provided a much closer fit, with RMSE range between 3.01-4.74 dB. Generally speaking, a model that provides a RMSE between 6-7 dB is considered a good fit [11].

The values in the urban area were very suspicious since it's expected that the path loss exponents will be higher than other areas. The explanation here is that 1 km intercept for an urban area may not be appropriate. The figure below shows downtown Tampa, which has a dense concentration of tall buildings. Here, an arbitrary center has been chosen, surrounded by a 1 km radius, the common intercept distance in this case. Most of the data within the area of the circle would be lost if the 1 km intercept distance was used. Also, it should be noted that cell radius is much smaller in the urban area than in the suburban and rural environment due to the lower antenna height.

Figure 18. Downtown Tampa.

The new filtered data shows a better agreement with the type of environment being studied as it will be shown in the next section.

4.4.4 Urban Environment Analysis and Model for Tampa Bay Area

Transmitters were set up in three different locations in downtown Tampa to collect RSS data. The data collected from these transmitters were originally analyzed not taking into consideration any filtering. As shown in Figure 18, to completely describe the environment within the downtown area, it is necessary to only consider data points within the area of interest. The table below shows the results of the path loss exponent of the sites located in the downtown area after filtering. The height of the sites ranged from 27-40 m.

Table 8. Path loss exponent comparison for transmitter located in downtown Tampa.

SITE	Path Loss Exponent Before Filtering Data	Path Loss Exponent After Filtering Data	100m-Intercept (dB)
SITE A	2.61	3.49	98.55
SITE B	2.43	4.93	102.60
SITE C	2.89	3.91	94.00

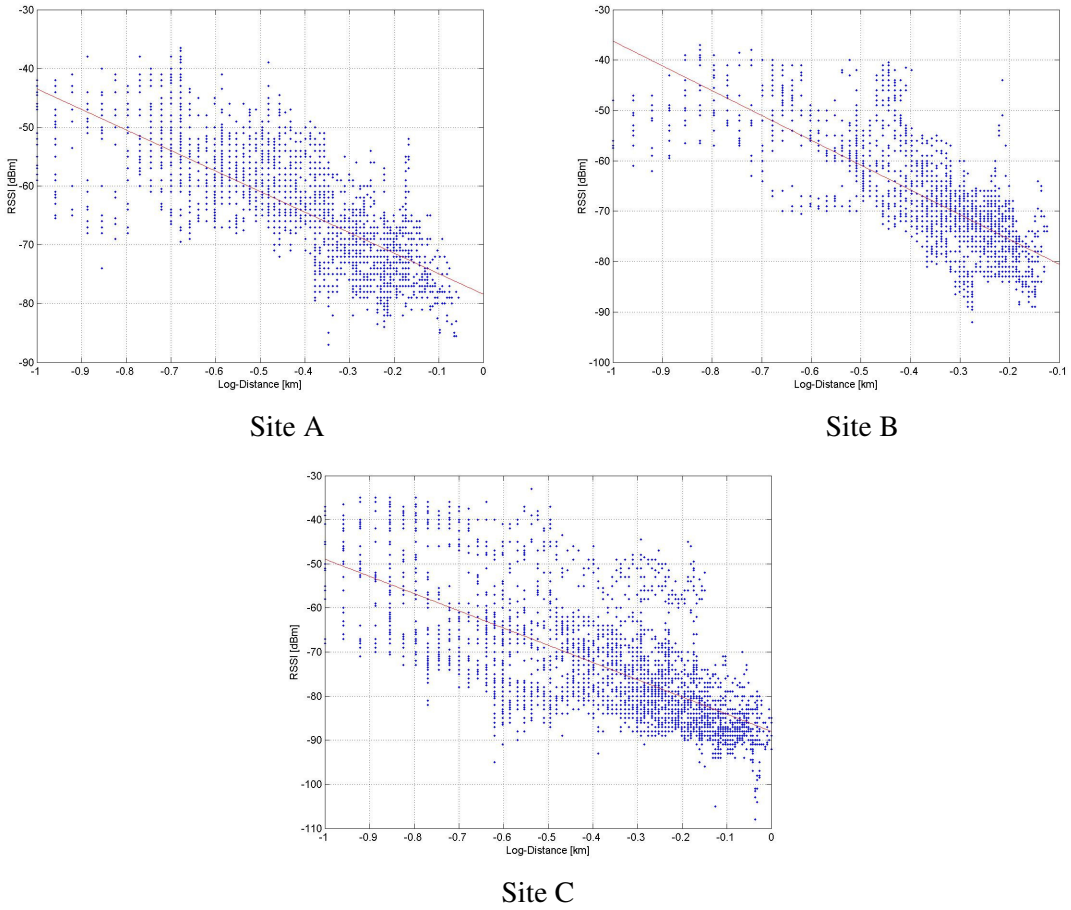

Site A

Site B

Site C

Figure 19. Regression analysis for sites in downtown Tampa.

The free space path loss for 2.6 GHz at 100 m is about 80.4 dB. The average measured path loss at 100 m for the sites in the downtown area was about 98 dB.

$$PL_o = 20\log_{10}\left(\frac{4\pi d_o}{\lambda}\right) \tag{31}$$

$$PL_{Urban\_Tampa} = 98.18 + 41.1\log_{10}\left(\frac{d}{d_o}\right) \tag{32}$$

Table 9. RMSE for urban environment sites in the Tampa Bay area.

SITE	Tampa Bay	COST-231
SITE A	6.9	11.49
SITE B	6.48	13.90
SITE C	7.22	8.09

The Tampa Bay model was compared against COST-231 and the RMSE is shown on Table 5. Since the SUI model does not have a profile for the urban environment, no comparison is made against the SUI model. The results of the new adapted model shows a better fit than the existing models. The difference between the models range from 0.8-7 dB.

CHAPTER 5

SHADOWING EFFECTS FOR TAMPA BAY AREA

Shadowing effects are very important for link budget purposes, handoff analysis, co-channel interference and frequency reuse studies, and diversity design. The main objective of this chapter is to explore the shadowing effects surrounding the Tampa Bay area, and to provide insight in the signal variation caused by terrain and other obstacles (which is also known as shadowing effect or slow fading).

5.1 Log-Normal Shadowing

Shadowing effects in empirical models are mainly described as a log-normal distribution [1]. The path loss at any distance from the transmitter can be described below.

$$PL(d)[dB] = \overline{PL}(d) + X_{\sigma} \tag{33}$$

Where X_{σ} is a zero-mean Gaussian distributed random variable (in dB) with standard deviation σ (also in dB).

The log-normal distribution describes the random shadowing effects. They occur over a large number of measurement locations which have the same distance separation between transmitter and receiver, but have different levels of clutter on the propagation path such as terrain irregularities, buildings, tress, etc.

Shadowing effects are shown simply by subtracting the best-fit path loss regression analysis from each individual measured local mean RSS values [12]. Some authors have described shadowing effects by histograms of excess path loss, which is the expected free space level minus the measured local mean [7]. The histogram showing this effect is shown in Figure 20 from one of the sites located in the Tampa Bay area. Similar patterns to other sites show the

same effect, confirming the shadowing effect is log-normally distributed. In addition, the plot in Figure 21 shows a linear fit superimposed on a sample of measured data. The straight-line fits show that shadowing effects come from a Gaussian distribution.

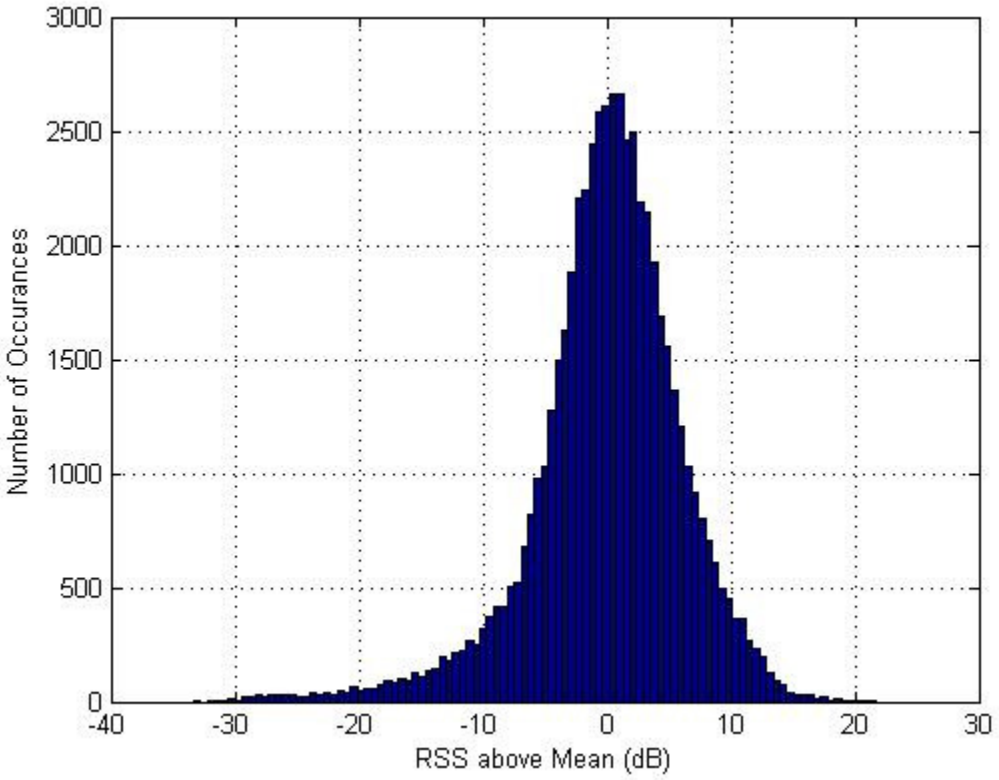

Figure 20. Log-normal distribution of shadowing effects. The data shows that shadowing effects appears to be Gaussian distributed as is commonly believed.

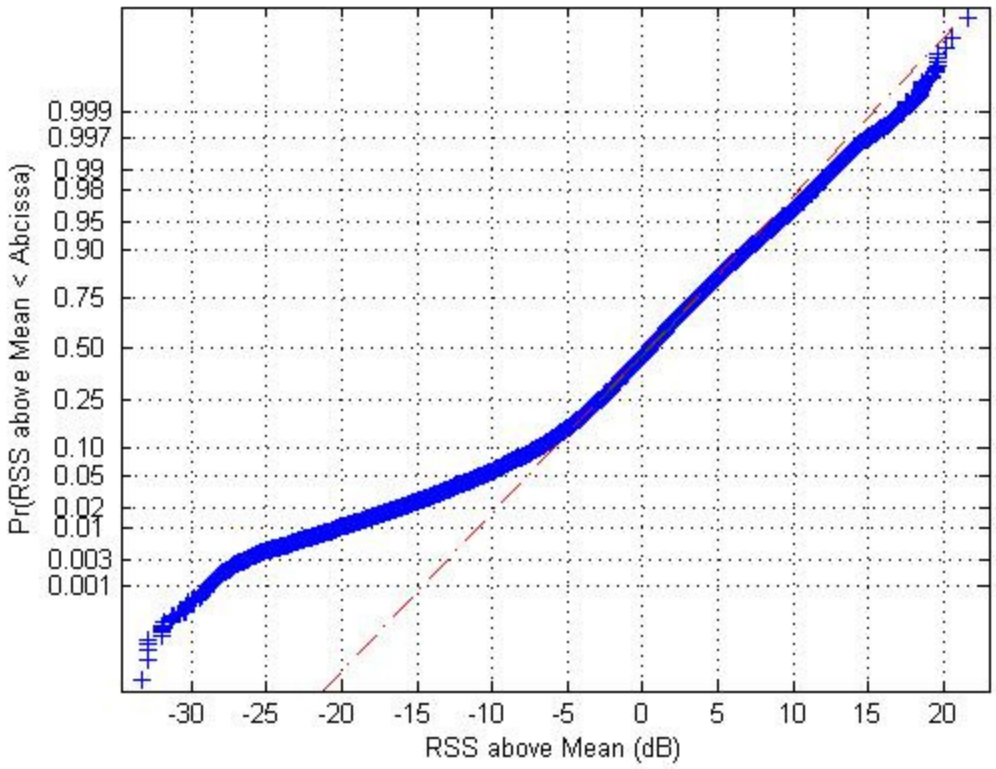

Figure 21. CDF of the shadowing fading components as a normal probability plot. The straight line fit shows that shadowing effects is near Gaussian.

5.2 Shadowing Effects Analysis for Tampa Bay Area

As expected, all sites analyzed in the Tampa Bay area showed a log-normal distribution about the mean distance dependent value as shown in Figure 20. In this section the techniques applied to determine the standard deviation σ for some of the suburban and urban sites will be discussed.

5.2.1 Data Analysis

In a mobile radio environment, the received signal envelope consists of large and small-scale fading phenomena. As mentioned before, this thesis is focused only on large scale fading, which is composed of distance dependent signal strength and variability of signal strength about the mean of the distance dependent RSS value. This variability is known as shadowing effects. Statistical analysis of shadowing effects require the removal of the distance dependence of RSS,

or path loss, in addition to the small scale fading as discussed in Chapter 3. In order to accomplish this, we simply subtract the best-fit path loss regression analysis from each individual measured local mean RSS values. Figure 20 shows the histogram of the shadowing effects components. As expected, the mean of this result appears to be concentrated around 0 dB with a standard deviation of about 8 dB.

Since the path loss in decibels is assumed to be a random variable with a normal distribution as shown in Equation (32), so is the RSS. The *Q*-function or error function (*erf*) may be used to the determine the probability that the received signal level will exceed (or fall below) a particular level. The *Q*-function is defined below.

$$Q(z) = \frac{1}{\sqrt{2\pi}} \int_{z}^{\infty} \exp\left(-\frac{x^2}{2}\right) dx = \frac{1}{2}\left[1 - erf\left(\frac{z}{\sqrt{2}}\right)\right] \tag{34}$$

The complementary *Q*-function is shown below.

$$Q(z) = 1 - Q(-z) \tag{35}$$

The probability that the RSS level (in dB) will exceed a certain value γ can be calculated from the cumulative density function as

$$P_r[P_r(d) > \gamma] = Q\left(\frac{\gamma - \overline{P_r(d)}}{\sigma}\right) \tag{36}$$

Similarly, the probability that the RSS level will be below γ is given by

$$P_r[P_r(d) < \gamma = Q\left(\frac{\overline{P_r(d)} - \gamma}{\sigma}\right) \tag{37}$$

Typical values for σ both for suburban and urban environments are shown on Table 10 and 11 respectively. The values are computed by calculating σ over distance increments from the transmitter to the receiver. In this case, σ was calculated over 1.6 km radius rings, and all values averaged over the total number of rings.

Table 10. Standard deviation in dB of suburban sites.

SITE	Standard Deviation
A	9.74
B	10.74
C	9.94
D	10.76
E	8.64
F	10.47

Table 11. Standard deviation in dB for urban sites.

SITE	Standard Deviation
A	9.74
B	10.72
C	13.41

5.2.2 Discussion

Originally it was suggested that σ was a function of distance. Since all values were calculated over 1.6-kilometer radius rings, this was easily accomplished. The work done by [13] suggested that for rural areas at 900 MHz, sigma varies with distance. To find the value of σ in dB, the following equations are presented for both radial routes σ_{LR} and circumferential routes σ_{LC} .

$$\sigma_{LR} \cong 3.0\log(d) + 6.0 \qquad 0.44 \le d \le 14 \tag{38}$$

$$\sigma_{LC} \cong 3.4\log(d) + 5.8 \qquad 0.44 \le d \le 14 \tag{39}$$

Where *d* is distance in kilometers.

Unfortunately, the data did not support a constant picture of this assumption, particularly for data points collected above 10 km as shown in Figure 22. This is due to the fact that enough was collected above 10 km.

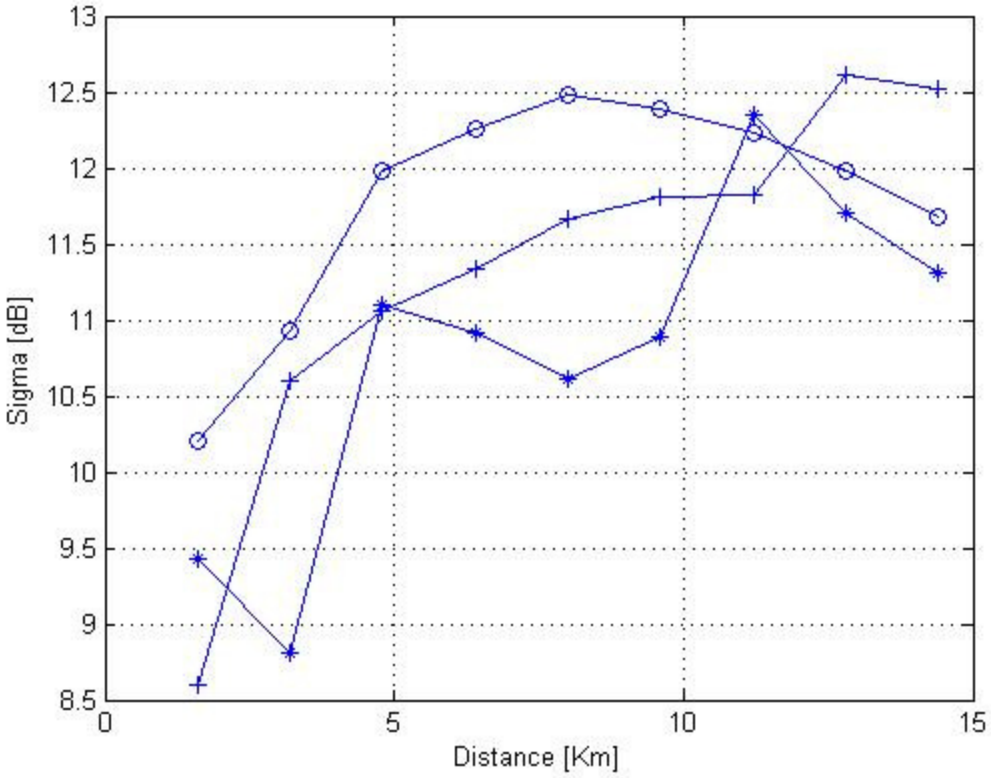

Figure 22. Shadowing effects as a function of distance. Sigma or the standard deviation describing shadow effects was first thought to be distance dependent. But not enough data was collected to get a constant picture, particularly for data points collected above 10 km.

5.3 Correlation Property Analysis for Tampa Bay Area

The log-normal process of shadowing effects described in the previous section is very useful in the performance analysis of handover procedures, the design of diversity schemes, and the study of the quality of service in mobile wireless systems. However, a better design of wireless systems can be accomplished by a better understanding of the spatial correlation properties of shadowing. In this section we do not propose a new model, but analyze the correlation properties of shadow effects in specific zones in the service area within the Tampa Bay area.

5.3.1 Spatial Correlation of Shadowing Effects

Models of spatial correlation properties of shadowing have been intensely studied since the classical paper of Gudmundson [14] has been published. Therein, the author proposes a simple exponential correlation model for shadowing effects.

$$R_A(k) = \sigma^2 a^{|k|} \tag{40}$$

$$a = \varepsilon_D^{v\,T/D} \tag{41}$$

Where R_A is the modeled normalized autocorrelation function, σ^2 is the variance, and ε_D is the correlation between two points separated by D. The signal is sampled every T second. Also, v is the mobile velocity and a is the correlation coefficient. This model is cited quite often in the literature when discussing the topic of correlation shadowing effects.

For typical suburban propagation at 900 MHz, it has been experimentally verified in [14] that σ is approximately 7.5 dB with a spatial correlation of about 0.82 at a distance of 100 m. For typical microcellular propagation at 1700 MHz, [14] shows that σ is approximately 4.3 dB with a spatial correlation of 0.3 at a distance of 10 m.

The correlation model described above assumes the mobile subscriber is moving in a straight line rather the along a closed route. A two-dimensional sum-of-sinusoids-based model for shadowing effects was introduced in [15]. The simulation of shadowing effects along a closed route involves more computational effort rather than along a straight line [16]. Therefore, in this section we analyze the correlation properties of shadowing effects along a closed route; that is, rings of specific widths. In the next section we review the properties of autocorrelation functions.

5.3.2 Autocorrelation Properties

The normalized autocorrelation function (NACF) is estimated by

$$\hat{\rho}(k) = \frac{\frac{1}{N}\sum_{n=0}^{N-k-1}(x(n)-\hat{m}_N)(x(n+k)-\hat{m}_N)}{\frac{1}{N}\sum_{n=0}^{N-1}(x(n)-\hat{m}_N)^2} \tag{42}$$

The function above is normalized to the variance of the measured data so as to constrain the values in the range -1 to 1. This function is used to calculate the correlation coefficients between one RSS data point to the next. This approach generates shadow effects variations that de-correlate exponentially with distance, but caution must be taken since it has been shown through extreme value analysis that log-normal shadows cannot de-correlate exponentially with distance by references in [17].

For the Tampa Bay area spatial correlation analysis, a function in MatLab called "xcorr" was used to exploit the autocorrelation properties of the received signal. This function is estimated for a sequence of *N* length and it is normalized so that the autocorrelation at zero lag is identical to 1.0.

$$\hat{R}_{xy}(k) = \sum_{n=0}^{N-1-k} x_{n+k}\, y_n, \qquad k = 0,1,\ldots,N-1 \tag{43}$$

The function above computes the autocorrelation for the special case of when *x*=*y*.

5.3.3 Data Analysis and Discussion

The following is a detailed analysis showing the correlation properties of RSS as it moves away from transmitter. This process uses concentric circles to determine the correlation between each incremented area. The plots below help identify correlation zones as the receiver moves away from the base station.

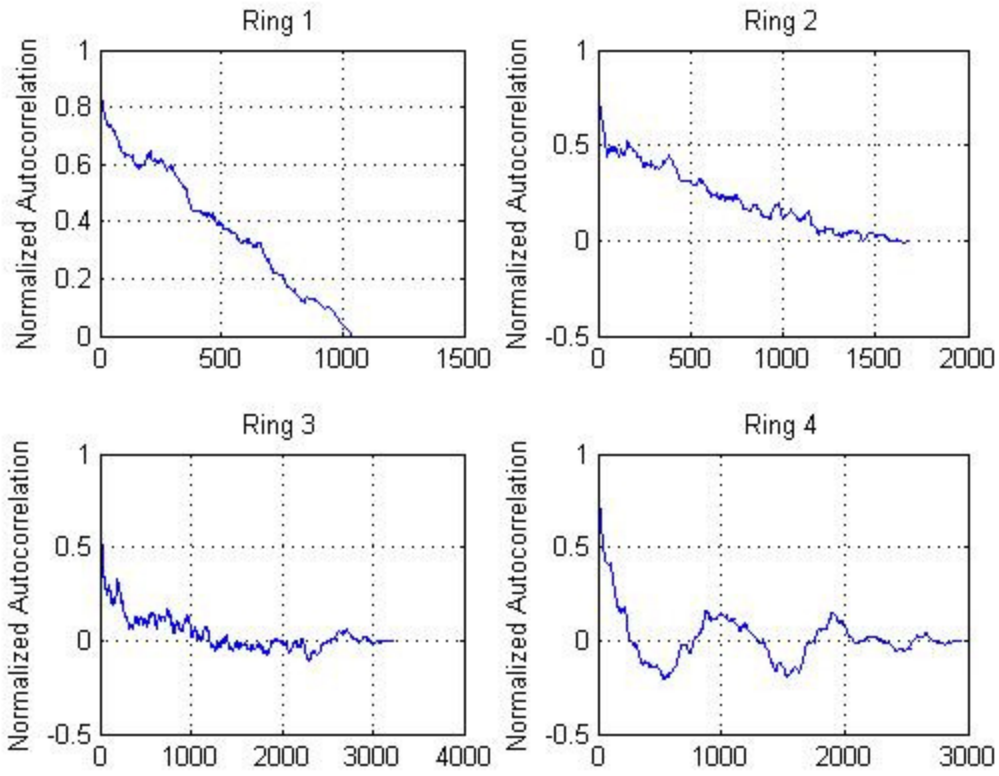

Figure 23. Normalized autocorrelation plots for ring 1. This represents shadow components between 1 to 1.32 kilometers, and the following rings are also incremented every 0.32 kilometer. Each sample in the abscissa represents 4.5 meters according to the sampling rate of the equipment. These rings have de-correlation distances between 100 and 1500 meters.

The basic method here is to collect data points within "donuts" or concentric circles of specific width – in this case 0.32 km. This width was selected so as to capture enough samples within each donut without losing possible information and correlation patterns.

Path loss effects were removed from each point by simply subtracting the measured value by the least square regression analysis of the data. The distance between each data point was calculated to be 4.5 m, based on the sampling rate of the equipment and frequency of interest.

In all the sites studied, a downward trend in low correlation patterns tends to occur close to the reference distance as it moves away from the transmitter.

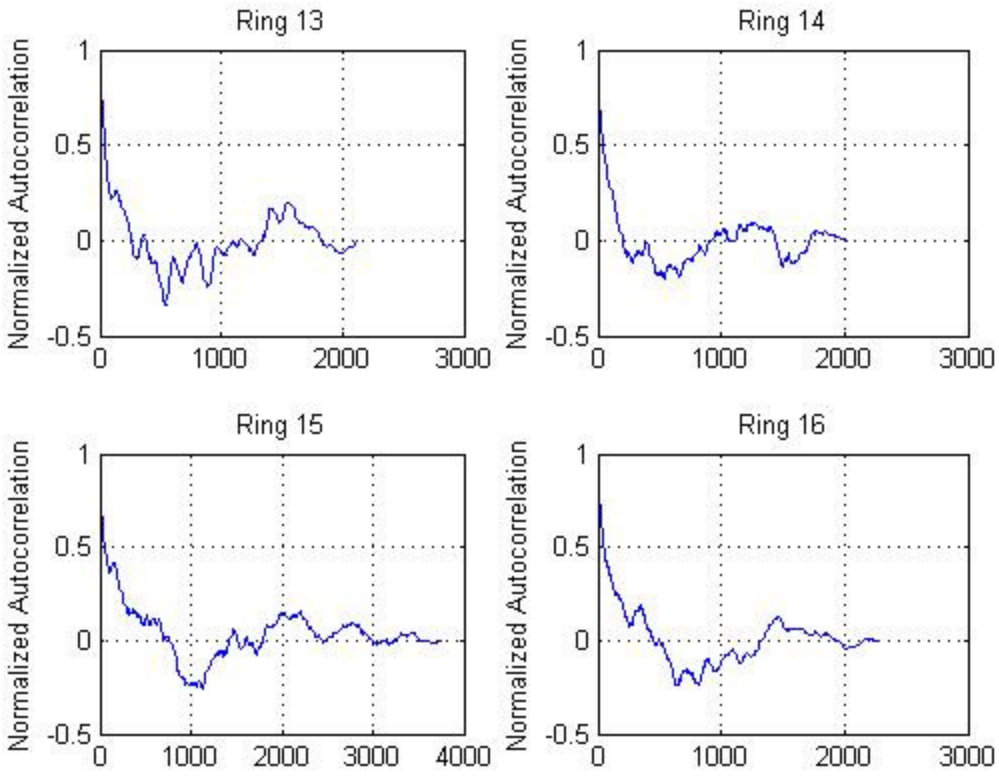

Figure 24. These rings suggest the existence of correlation zones. The shadow effects components seem to behave equally and he de-correlation distances on the figures above range from 185 to 207 m.

When objects are closer to the receiver, such as buildings, severe shadow can occur and the signal may go into deep fade. The effect is observed in Figure 24. The non-periodic correlation tends to occur between the low correlation and slow correlation zones. These patterns are observed to have fairly high peaks from the zero lag which may be due to effects of street orientation.

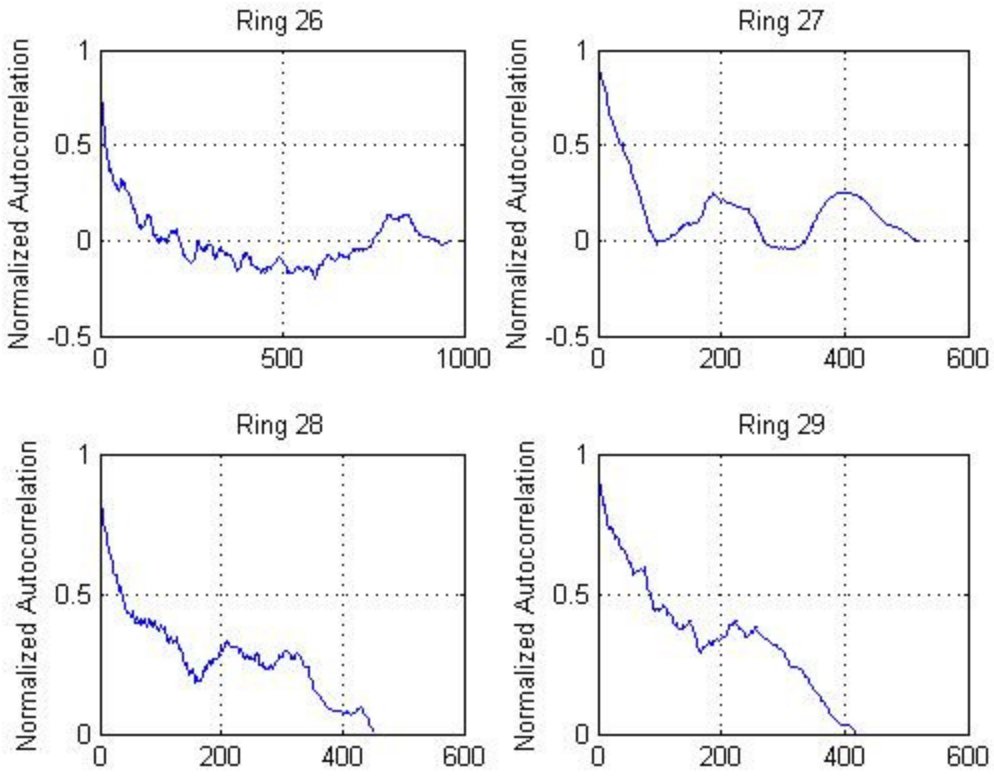

Figure 25. These rings are the farthest away from the transmitter. They are approximately 10 kilometers away from the transmitter, and de-correlation distances on the figures above range from 63 to 378 m.

Particularly in urban areas it has been observed [17] that the radio signal tends to be channeled by the buildings so that a tunnel effect (stronger signal are not necessary line of sight) occurs. Median received signal strength can vary by as much as 20 dB when near the transmitter station. Slow correlation tends to occur when shadowing objects are not close to the receiver. This phenomenon is observed particularly far from the base station as seen in Figure 25.

CHAPTER 6

CONCLUSION

Improvement of accuracy of propagation models will continue to be an integral part of wireless communication systems. This will be even more apparent with the recent convergence of mobile cellular networks and the Internet. In this thesis the propagation characteristics of the wireless channel in the 2.6 GHz frequency band around the Tampa Bay area are studied. It is shown that an adapted model based on the logarithmic path loss model provides a better fit than existing empirical models. The shadowing effects were studied in detail and the spatial correlation of shadowing effects was investigated.

6.1 Contributions

The main contribution of this thesis was to share some insight on the propagation characteristic of the radio link in the Tampa Bay area. Adapted models for suburban and urban zones within the Tampa Bay area were presented, including a specific adapted model to support bridges in the Tampa Bay area. These models will help to more accurately predict coverage and interference within the area, particularly along the major bridges in the Tampa Bay area. The proposed adapted methods provide a much better fit than any other existing model, however it is specific for Tampa Bay. Additionally, the log normal distribution and spatial correlation properties of shadowing effects were discussed. The spatial correlation properties of the normalized RSS were exploited in detail using concentric zones.

6.2 Future Work

The path loss and correlation analyses in this thesis highlight on how the radio signal propagates in the Tampa Bay area. These studies can be used to compare future path loss and

correlation models. Specifically, correction factors for antenna height can be developed. Also, the path loss analysis studied in this thesis could be added as a possible terrain profile to existing models, particularly to the SUI model. In addition, it would be interesting to discover a simple spatial correlation function that describes the correlation zones investigated in Chapter 5.

REFERENCES

[1] Rappaport, T. S., *Wireless Communications Principles and Practices,* 2nd Edition, Prentice Hall PTR, Upper Saddle River, NJ 2002

[2] Whitteker, J.H., "Physical optics and field-strength predictions for wireless systems," *Selected Areas in Communications, IEEE Journal on*, vol.20, no.3, pp.515-522, April 2002

[3] Hata, M., "Empirical formula for propagation loss in land mobile radio services," *Vehicular Technology, IEEE Transactions on*, vol.29, no.3, pp. 317-325, August 1980

[4] Erceg, V.; Greenstein, L.J.; Tjandra, S.Y.; Parkoff, S.R.; Gupta, A.; Kulic, B.; Julius, A.A.; Bianchi, R., "An empirically based path loss model for wireless channels in suburban environments," *Selected Areas in Communications, IEEE Journal on*, vol.17, no.7, pp.1205-1211, July 1999

[5] Erricolo, D.; Uslenghi, P.L.E., "Propagation path loss-a comparison between ray-tracing approach and empirical models," *Antennas and Propagation, IEEE Transactions on*, vol.50, no.5, pp.766-768, May 2002

[6] Giovaneli, C.L., "An analysis of simplified solutions for multiple knife-edge diffraction," *Antennas and Propagation, IEEE Transactions on*, vol.32, no.3, pp. 297-301, March 1984

[7] Jakes, C.W. *Microwave Mobile Communications*, IEEE Press, Piscataway, NJ, 1993

[8] Lee, W.C.Y., "Estimate of local average power of a mobile radio signal," *Vehicular Technology, IEEE Transactions on*, vol.34, no.1, pp. 22-27, February 1985

[9] Min, S.; Bertoni, H.L., "Effect of path loss model on CDMA system design for highway microcells," *Vehicular Technology Conference, 1998. VTC 98. 48th IEEE* , vol.2, no.3, pp.1009-1013, May 1998

[10] Wittink, D. R. *The Application of Regression Analysis*, Allyn and Bacon, Inc., Needhan Heights, Massachusetts, 1988

[11] Parsons, J.D. *Mobile Radio Propagation Channel*, Wiley, Chichester, West Sussex, England, 1992

[12] Steele, R. *Mobile Radio Communications*, IEEE Press, New York, 1992

[13] Mockford, S.; Turkmani, A.M.D.; Parsons, J.D., "Local mean signal variability in rural areas at 900 MHz," *Vehicular Technology Conference, 1990 IEEE 40th*, vol., no., pp.610-615, 6-9 May 1990

[14] Gudmundson, M., "Correlation model for shadow fading in mobile radio systems," *Electronics Letters*, vol.27, no.23, pp.2145-2146, 7 November 1991

[15] Xiaodong Cai; Giannakis, G.B., "A two-dimensional channel simulation model for shadowing processes," *Vehicular Technology, IEEE Transactions on*, vol.52, no.6, pp. 1558-1567, November 2003

[16] Patzold, M.; Nguyen, V.D., "A spatial simulation model for shadow fading processes in mobile radio channels," *Personal, Indoor and Mobile Radio Communications, 2004. PIMRC 2004. 15th IEEE International Symposium on*, vol.3, no.3, pp. 1832-1838, September 2004

[17] Stuber, G. L., *Principles of Mobile Communication,* 2nd Edition, Kluwer Academic, Norwell, Massachusetts, 02061